Am J Transl Res 2024;16(6):2248-2262
www.ajtr.org /ISSN:1943-8141/AJTR0154841

Original Article

Huangtu decoction alleviates chronic diarrhea of spleen-yang deficiency in mice by altering host metabolome and intestinal microbiota composition

Wenwen Chen[1*], Chunyan Huang[2*], Dandan Tang[3], Jun Wan[4], Xia Zhou[4], Chunjie Wu[2], Xiao Yang[5]

[1]Department of Pharmacy, Chengdu Women's and Children's Central Hospital, School of Medicine, University of Electronic Science and Technology of China, Chengdu 610091, Sichuan, China; [2]Department of Quality Assurance and Scientific Research, Chengdu Institute for Drug Control, Chengdu 610045, Sichuan, China; [3]School of Pharmacy, Chengdu University of Traditional Chinese Medicine, Chengdu 611137, Sichuan, China; [4]College of Life Science and Engineering, Southwest Jiaotong University, Chengdu 610031, Sichuan, China; [5]Department of Obstetrics, Chengdu Women's and Children's Central Hospital, School of Medicine, University of Electronic Science and Technology of China, Chengdu 610091, Sichuan, China. [*]Equal contributors.

Received December 8, 2023; Accepted May 6, 2024; Epub June 15, 2024; Published June 30, 2024

Abstract: Background: *Huangtu* decoction (HTD), a traditional Chinese medicine recipe, warms the spleen, nourishes the blood, and stops bleeding. It has been used to treat dysentery, gastrointestinal bleeding, diarrhea, and other symptoms caused by spleen-yang deficiency for more than 2,000 years in China. However, the mechanism underlying the treatment of chronic diarrhea due to spleen-yang deficiency (CDSD) using HTD remains unclear. Aims: This study investigated whether HTD could mediate intestinal flora and serum metabolites to improve CDSD symptoms using a mouse model. Methods: A CDSD mouse model induced by senna and an abnormal diet was constructed. The regulatory effects of HTD at 12.5, 25.0, and 50.0 g/kg/d on CDSD mice were assessed by measuring their bodyweight, diarrhea rate, loose stool rate, and histopathology. Changes in the intestinal flora of CDSD mice were analyzed by 16S rRNA gene sequencing. Untargeted serum metabolomic analysis was performed using ultra-high performance liquid chromatography-mass spectrometry/mass spectrometry (UHPLC-MS/MS). Results: HTD had a modulating effect on CDSD by reducing the weight loss, diarrhea rate, loose stool rate, and pathologic damage. Intestinal flora analysis showed that HTD altered the community composition by decreasing the abundance of Allobaculum, Lactobacillus, and Ruminococcus. Serum metabolomics revealed that ascorbate and aldarate metabolism, aldosterone synthesis and secretion, platelet activation, hypoxia-inducible factor 1 signaling pathway, inositol phosphate metabolism, phosphatidylinositol signaling, galactose metabolism, and alpha-linolenic acid metabolism were modulated after HTD treatment. Conclusion: HTD may alleviate CDSD symptoms by reducing weight loss, diarrhea rate, loose stool rate, and pathologic damage caused by modeling and regulating intestinal flora and serum metabolites in CDSD mice.

Keywords: *Huangtu* decoction, chronic diarrhea, metabolomes, intestinal microbiotas, traditional Chinese medicine, antidiarrheal

Introduction

Chronic diarrhea is a common gastrointestinal disorder with a global prevalence of 3-20% and is a public health problem in many regions of the world, especially where poverty prevails [1, 2]. Children in poor countries are at a higher risk of developing diarrhea [3]. Globally, approximately 530,000 children under five years old died from diarrhea in 2017, accounting for approximately 78.4 per 100,000 [4]. Chronic diarrhea severely affects quality of life, leads to high healthcare utilization, and incauses a financial burden [5].

Evidence suggests that the gut microbiome is closely related to diarrhea and that the composition of the intestinal microbial community could provide a phenotypic marker of human susceptibility to diarrheal disease [6-8]. Fecal microbiota transplantation is expected to become a new treatment for diarrhea [9]. The

https://doi.org/10.62347/IHNX2675

intestinal microbiome can also affect the development of diseases by affecting the host metabolites [10, 11].

The acceptance of traditional Chinese medicine (TCM) has gradually increased world wide. In subjects with IBS, the gut microbiota has been observed to have increased levels of Enterobacteriaceae, Ruminococcus, Clostridium, and Dorea species and decreased levels of Lactobacillus, Bifidobacterium, and Faecalibacterium species compared to healthy controls [12, 13]. The discovery of new therapeutic drugs from TCM has become a research hotspot [14]. TCM treatment is a complementary and alternative therapy for diarrhea with a good curative effect [15-17]. Some studies have indicated that herbs and recipes from TCM used to treat diarrhea could also improve the structure and function of intestinal flora [18-20].

In TCM, "spleen" is different from the anatomical spleen organ. It is a comprehensive concept of structures mainly involving the spleen, stomach, pancreas, and lymphoid [17]. The spleen is the hub for digesting food, distribution of cereal essence, and body fluid metabolism, and it has a close relationship with maintaining the basic functions of the human body [21]. Spleen yang deficiency disturbs the gastrointestinal movement, and is clinically manifested by loss of appetite, indigestion, weight loss, abdominal distension, and loose stools or diarrhea [22].

Huangtu decoction (HTD) is a well-known TCM recipe that has been used for over 2,000 years in China to treat dysentery, bloody stools, and diarrhea caused by spleen-yang deficiency with a good effect [23]. However, there is little research and development on this classic recipe. It is composed of seven medicinal herbs: *Terra Flava Usta*, *Rehmanniae Radix, Scutellariae Radix*, *Aconiti Lateralis Radix Praeparata*, *Asini Corii Colla*, *Atractylodis Macrocephalae Rhizoma,* and *Glycyrrhizae Radix et Rhizoma*. In our previous study, HPLC-MS/MS was used to analyze the chemical compositions of HTD, and a total of 47 compounds were identified from it, mostly flavones and alkaloids, such as LicoricesaponinG2, Glycyrrhizic Acid, Liquiritigenin, Wogonin, Eriodictyol, Luteolin, Quercetin, Genistein, Pinobanksin, Hesperetin, Isorhamnetin, Chrysin, Pinocembrin, Calycosin, Retrochalcone, 5-Hydroxymethyl-2-Furaldehyde, Atractylenolide III, Uridine, Adenosine, Phlinoside A, Rehmannioside D, Citric Acid, Guanosine, Mussaenosidic Acid, Verbascoside, Martynoside, P-Coumaric Acid, Vanillic Acid, 4-Hydroxybenzoic Acid, Scutellarin, Apigenin-7-O-Glucuronide, 2', 5,6',7-Tetrahydroxyflavanone, Karakoline, Isotalatizidine, Fuziline, Talatizamine, Neoline, Songorine, Aconine, Hetisine, Benzoylmesaconine, 14-Benzoylaconine, Benzoylhypaconine, Mesaconitine, Hypaconitine, Aconitine, and Deoxyaconitine [23]. However, the mechanism of HTD in the treatment of diarrhea is still not clear.

In this study, we constructed a CDSD mice model to investigate the regulative role of HTD on intestinal flora and serum metabolites. The CDSD mice model was induced by the combination of laxative and irregular diet, which was similar to the syndrome of "spleen-yang deficiency" diarrhea. All the mice had diarrhea, accompanied by withered fur, poor mental appetite, and little aggregation, indicating that the CDSD modeling was successful. The criteria for diagnosing spleen-yang deficiency syndrome diarrhea in mice, based on macroscopic symptoms, include: watery stools or unformed fecal pellets, cold limbs, a hunched back, reduced food intake and weight loss, along with signs of lethargy. These diagnostic guidelines are derived from the clinical signs of spleen-yang deficiency syndrome diarrhea and relevant literature references.

Materials and methods

Preparation of drug extract

HTD extracts were prepared according to the method described by 'JingGuiYaoLue'. Briefly, seven herbs *Terra Flava Usta* (111.4 g, AnguoJuyaotang Pharmaceutical, CHN), *Rehmanniae Radix* (41.8 g, Sichuan Neautus TCM, CHN), *Scutellariae Radix* (41.8 g, Sichuan Neautus TCM, CHN), *Aconiti Lateralis Radix* Praeparata (41.8 g, Sichuan Neautus TCM, CHN), *Asini Corii Colla* (41.8 g, Sichuan Neautus TCM, CHN), *Atractylodis Macrocephalae Rhizoma* (41.8 g, Sichuan Neautus TCM, CHN), and *Glycyrrhizae Radix et Rhizoma* (41.8 g, Sichuan Neautus TCM, CHN) were mixed with purified water. *Aconiti Lateralis Radix Praeparata* were soaked for 12 h. The other herbs were soaked for 30 min, boiled twice for 1 h, filtered, and concentrated to 2 g/mL of decoction.

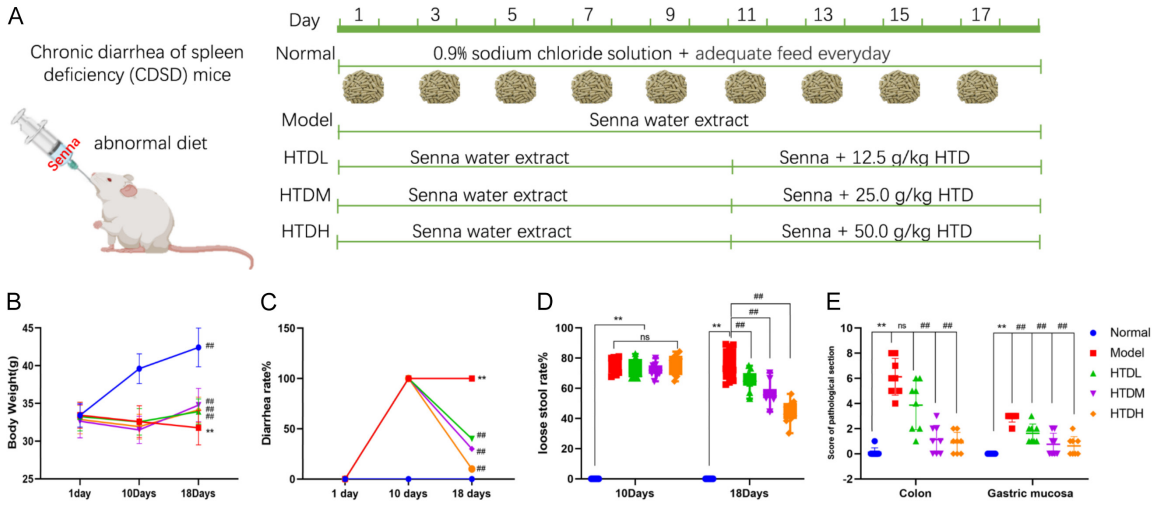

Figure 1. Effect of HTD on CDSD mice induced by senna water extract and abnormal diet (n = 10). A. Schematic diagram of CDSD mice establishment and HTD treatment. B-E. HTD significantly reduces the weight loss, diarrhea rate, loose stool rate, and pathologic damage of colonic and gastric mucosa in CDSD mice. Values are expressed as mean ± SD. **P < 0.01 vs. Normal group. ##P < 0.01 vs. Model group.

Senna water extract: Senna leaves (100 g, Sichuan Neautus TCM, CHN) were soaked in warm water for 12 h. The residue was filtered and concentrated to 100 mL to obtain a 1 g/mL concentration of senna water extract and then stored at 4°C.

Animals and experimental design

Specific pathogen-free (SPF)-grade male Kunming (KM) mice (22-28 g) were supplied by SPF (Beijing) Biotechnology Co., Ltd. (DCXK (Beijing) 2019-0010). The mice were kept in independent ventilation cages at a constant temperature (22 ± 2°C) and humidity (55 ± 10%) with 12 h of light per day and allowed food and water ad libitum for 7 days before the experiment.

A total of 50 KM mice were randomly and equally divided into 5 groups: the normal group, model group, HTD-treated low-dose group (12.5 g/kg, HTDL), HTD-treated medium-dose group (25.0 g/kg, HTDM), and HTD-treated high-dose group (50.0 g/kg, HTDH). Chronic diarrhea of spleen-yang deficiency (CDSD) mice was induced by feeding in a cycle of full food for 1 d, fasting for 1 d, with 0.04 mg/kg senna water extract every day according to body weight for 10 days [17, 24-27]. After modeling, the CSCD mice exhibited different degrees of symptoms, including diarrhea, darkening of fur, loss of appetite and weight, and laziness, indicating that the modeling was successful. Saline was administered to the normal group. The CDSD mice were treated with HTD extract for 7 days at an arranged dose, except for the model group. Finally, all the mice were fasted overnight for at least 12 h and were sacrificed following isoflurane anaesthesia the next day (**Figure 1A**). The serum, colon tissues, gastric mucosa, and feces were collected for further analysis. The weight, diarrhea rate, loose stool rate, and pathological damage of colon and gastric mucosa of each group were analyzed (**Figure 1B-E**).

The animal experimental protocol was approved by the Ethics Review Committee of Chengdu Women's and Children's Central Hospital (No. [2023]6, 2023/01/16). All procedures were performed in accordance with the Guide for the Care and Use of Laboratory Animals (National Institute of Health).

Body weight, diarrhea rate, and loose stool rate

The weight, number of loose stools, total stools within 6 h after administration, and number of diarrhea mice in each group were recorded at the 1, 10, and 18 days of the experiment. The diarrhea and loose stool rates were calculated using the following formula:

$$\text{Diarrhea rate} = \frac{\text{number of diarrhea mice in each group}}{\text{total number of mice in each group}} \times 100\%;$$

$$\text{Loose stool rate} = \frac{\text{number of loose stools within 6 hours after administration}}{\text{total number of stools within 6 hours after administration}} \times 100\%.$$

Table 1. Histopathologic scoring criteria of colonic and gastric mucosa

Score		0	1	2	3
Colon	Epithelial injury and ulcer	-	Erosion	Ulcer (involving mucosa and submucosa)	Ulcer (involving mucous muscularis to the serosa)
	Edema and congestion	-	Mild	Moderate	Severe
	Lymphoid, mononuclear, and plasma cell infiltration	-	Mild	Moderate	Severe
	neutrophil infiltration	-	Mild	Moderate	Severe
	Eosinophil infiltration	-	Mild	Moderate	Severe
	Gland damage	-	Mild	Moderate	Severe
Gastric mucosa	Inflammation and mucosal damage	-	Local congestion, redness, and other mild damage	epithelial detachment, focal erosion, and other moderate damage	Massive bleeding, erosion (> 2 mm), and other severe damage

Histopathology

The colon and stomach samples were cut into small pieces, fixed in 4% paraformaldehyde, embedded in paraffin, and stained with hematoxylin and eosin (H&E). Histopathologic changes were examined under a microscope and scored according to specific criteria, as shown in **Table 1**.

Genomic DNA extraction and 16S rRNA sequencing

The feces were collected from the colon of mice, placed in sterile tubes, and immediately frozen at -80°C. Genomic DNA extraction and 16S rRNA sequencing of the normal, model, and HTDM groups was performed by Novogene Co., LTD. The cetyl trimethylammonium bromide method was used for faecal DNA extraction. The purity and concentration of the DNA were detected by agarose gel electrophoresis, and diluted to 1 ng/μl. The 16S rRNA genes of the V4 region were amplified using the 515F-806R primer with a barcode. All polymerase chain reactions (PCR) were conducted with the Phusion® High-Fidelity PCR Master Mix (New England Biolabs) on a Bio-Rad T100 gradient thermal cycler. Finally, the library was sequenced on an Illumina NovaSeq platform, and 250 bp paired-end reads were generated.

Sequencing data analysis

Effective tags were obtained after merging the paired-end reads of each sample using FLASH (V1.2.7) software [28], filtered using QIIME (V1.9.1 [29]), and the chimeric sequences were removed. Sequence analysis was performed using Uparse (v7.0.1001) [30] and sequences with ≥ 97% similarity were assigned to the same operational taxonomic units (OTUs). The representative sequence for each OTU was screened for further annotation using the Silva database [31], which was based on the Mothur algorithm to annotate taxonomic information. The unweighted pair-group method with arithmetic mean clustering was performed using QIIME (Version 1.9.1). Linear discriminant analysis Effect Size (LEfSe) analysis was performed using the LEfSe software with the default setting of a screening value of 4 for the LDA score. 3D Principal component analysis (PCA) plots, principal coordinate analysis (PCoA) plots, and plots of significant differences in species between groups were created using R (version 2.15.3).

Serum metabolomics assays

The serum samples were mixed and resuspended in prechilled 80% methanol and 0.1% formic acid by vortexing. Then the samples were incubated on ice for 5 min and centrifuged at 15,000 g, 4°C for 20 min. Some of the supernatants were diluted to a final concentration containing 53% methanol by LC-MS-grade water. Subsequently, the samples were centrifuged at 15,000 g, 4°C for 20 min. Finally, the supernatant was injected into the UHPLC-MS/MS system analysis [32].

UHPLC-MS/MS analyses were performed using a Vanquish UHPLC system (Thermo Fisher, Germany) coupled with an Orbitrap Q Exactive™ HF mass spectrometer (Thermo Fisher, Germany) in Novogene Co., Ltd. (Beijing, China). Chromatographic conditions: Hypesil Gold column (100×2.1 mm, 1.9 μm), 40°C, a flow rate of 0.2 mL/min, and a 17-min linear gradient

were applied. The eluents for the positive polarity mode were eluent A (0.1% formic acid in water) and eluent B (methanol), whereas the eluents for the negative polarity mode were eluent A (5 mM ammonium acetate, pH 9.0) and eluent B (methanol). The solvent gradient was set as follows: 2% B, 1.5 min; 2-100% B, 12.0 min; 100% B, 14.0 min; 100-2% B, 14.1 min; 2% B, 17 min. Q Exactive™ HF mass spectrometer was operated in positive/negative polarity mode with a spray voltage of 3.2 kV, capillary temperature of 320°C, sheath gas flow rate of 40 arb, and auxiliary gas flow rate of 10 arb.

Metabolomic data analysis

To obtain accurate qualitative and relative quantitative results for each metabolite, the raw data files generated by UHPLC-MS/MS were processed using the Compound Discoverer 3.1 (CD3.1, Thermo Fisher) to obtain accurate qualitative and relative quantitative results for each metabolite. PCA and partial least squares discriminant analysis (PLS-DA) were performed using metaX [33]. Metabolites with a VIP > 1 and *P*-value < 0.05 and fold change ≥ 2 or FC ≤ 0.5 were recognized to as differential metabolites. Metabolites were annotated using the KEGG, HMDB, and LIPID MAPS databases. Univariate analysis (t-test) was performed to determine the statistical significance (*p*-value). Volcano plots and heatmaps were generated in the R language. Pearson's correlation between differential metabolites was assessed using the cor() function in R language. Metabolic pathway enrichment of the differential metabolites was assessed using the KEGG database. If x/n > y/N, the metabolic pathway was identified as being enriched. Statistical significance (*P*-value) was calculated by univariate analysis (*t*-test), and *P*-values < 0.05 were considered significant. MetaStat analysis was performed at each taxonomic level to obtain *P* values for the permutation test between the groups.

Results

Physical and physiologic effects of HTD in CDSD mice

The diarrhea assessment results revealed that weight loss, diarrhea rate, and loose stool rate were significantly higher (P < 0.01) in the model group than in the control and HTD treatment groups (**Figure 1B-D**). Compared to the control group, H&E staining revealed obvious pathologic changes in the colon and gastric mucosa in the model group; however, HTD treatment could reduce these pathologic changes with a dose-dependent effect (**Figure 2**).

Intestinal flora diversity analysis of mice in different groups

As shown in **Figure 3A**, the overall structural characteristics of the intestinal flora of the three groups were compared using PCoA (**Figure 3A**), Venn diagram (**Figure 3B**), and unweighted pair-group method with arithmetic mean dendrogram (**Figure 3C**). The model group was distant from the normal group. In contrast, the HTD group was clustered together, indicating that the intestinal flora of CDSD mice was significantly altered, and the composition of intestinal flora became similar to that of healthy mice after HTD administration. The overlapping part in Venn showed that 478 OTUs were common among the three groups, and the specific OTUs in the normal, model and HTD groups were 27, 38, and 30, respectively. **Figure 3D-F** shows the relative abundance of the top ten intestinal flora at the phylum, family, and genus levels. The ternary diagram profiles in **Figure 3G-I** show the dominant OTU differences among groups.

The top ten most abundant phyla in the normal group were mainly composed of Bacteroides and Firmicutes. Compared to the normal group, the abundance of Campilobacterota (P < 0.05) and Proteobacteria (P < 0.01) in the model group increased significantly, while the abundance of Actinobacteria (P < 0.05) and Cyanobacteria (P < 0.05) decreased significantly. No significant differences were found between the HTD and model groups at the phylum level (**Figure 4A**). At the family level, the intestinal flora of the normal group mice was mainly composed of Muribaculaceae, Bacteroidaceae, Staphylococcaceae, Erysipelotrichaceae, Prevotellaceae, Lachnospiraceae, Corynebacteriaceae, and Akkermansiaceae. Compared to the normal group, the relative abundances of Staphylococcaceae (P < 0.05) and Corynebacteriaceae (P < 0.05) in the model group were significantly lower, whereas those of Bacteroidaceae (P < 0.05), Erysipelotrichaceae (P < 0.01), and Lactobacillaceae

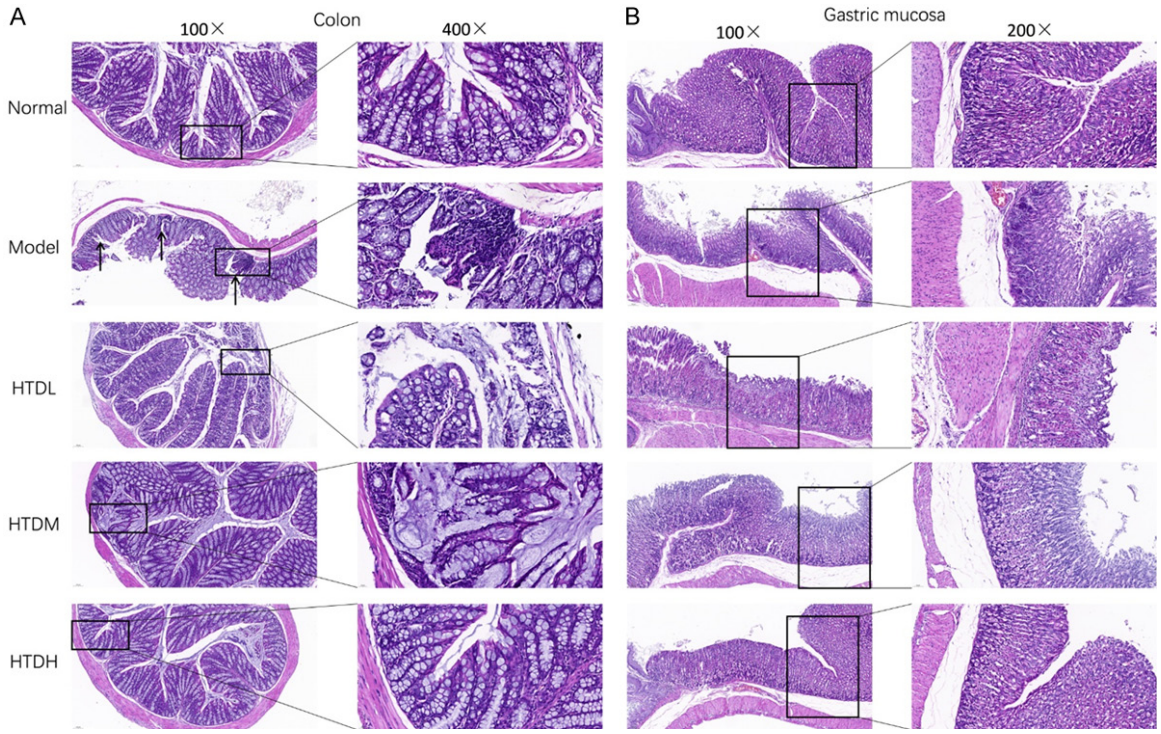

Figure 2. Histopathologic examination of the colonic and gastric mucosa in CDSD mice. A. H&E staining of the colon (n = 8). B. H&E staining of the gastric mucosa (n = 8).

($P < 0.05$) were higher. Compared to the model group, the abundance of Erysipelotrichaceae ($P < 0.01$) and Lactobacillaceae ($P < 0.05$) was significantly lower in the HTD group (**Figure 4B**). At the genus level, the intestinal flora of the normal group mice was mainly composed of Bacteroides, Staphylococcus, Allobaculum, Alloprevotella, and Corynebacterium. Compared to the normal group, the abundance of Blautia ($P < 0.05$), Helicobacter ($P < 0.01$), Bifidobacterium ($P < 0.01$), Parasutterella ($P < 0.01$), Bacteroides ($P < 0.05$), Lactobacillus ($P < 0.05$), Allobaculum ($P < 0.01$), Rikenellaceae RC9 ($P < 0.05$), and Roseburia ($P < 0.05$) were significantly higher, while Corynebacterium ($P < 0.05$), Jeotgalicoccus ($P < 0.05$), Staphylococcus ($P < 0.01$), Aerococcus ($P < 0.01$), Rikenella ($P < 0.05$), Alistipes ($P < 0.01$) were lower. Compared to the model group, the abundance of Allobaculum ($P < 0.01$) and Lactobacillus ($P < 0.05$) in the HTD group decreased significantly, and the abundance of Ruminococcus ($P < 0.01$) increased significantly (**Figure 4C**). In addition, we performed LEfSe analysis and plotted a cladogram (**Figure 4D**, **4E**), which allowed us to determine that the model group-specific flora included Allobaculum. The model group-specific flora were significantly reduced after HTD administration.

Differential metabolite and pathway analysis in mice

The serum metabolome was analyzed to identify differential metabolites in CDSD mice after HTD treatment. First, PCA and PLS-DA analyses were performed on the three groups of serum samples to visualize the overall metabolite changes (**Figure 5A**, **5B**, **5E**, **5F**). The results showed that the normal *vs*. model groups differed significantly in the 3D PCA and PLS-DA score plots, indicating that the CDSD mouse model was successfully built. In contrast, the metabolites of mice treated with HTD were significantly altered compared to the model group, suggesting that HTD altered the abnormal metabolic profile of CDSD mice. A volcano plot was used to visualize the overall distribution of metabolite differences between the groups (**Figure 5C**, **5G**). In addition, correlations between these differential metabolites were analyzed (**Figure 5D**, **5H**). The correlation of the differential metabolites indicated that 99 metabolites were negative and 82 were positive in the normal *vs*. model groups.

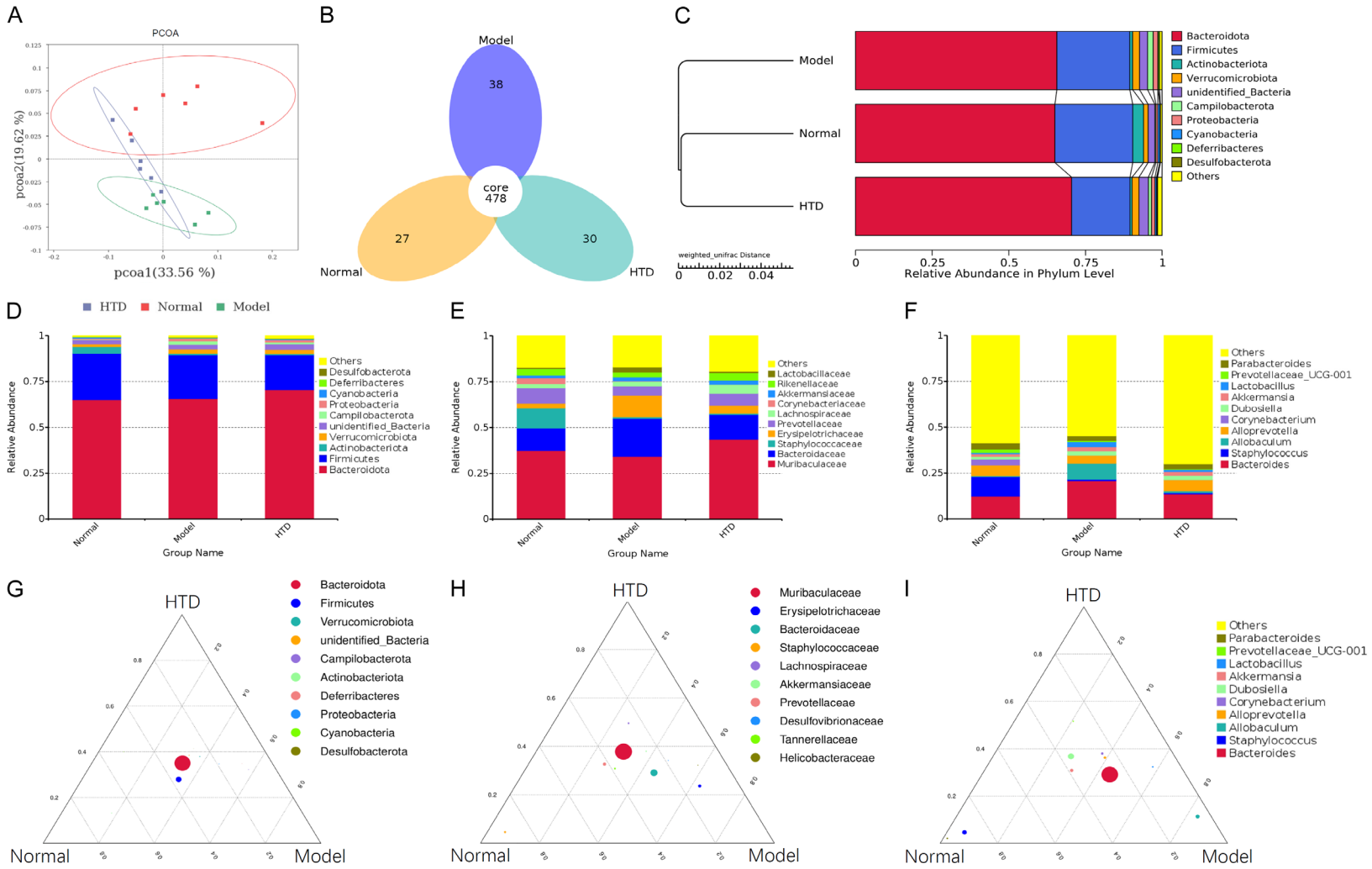

Figure 3. Analysis of intestinal flora composition of mice in each group. A. PCoA, based on weighted uniFrac distance, shows the beta diversity of each group. B. Venn diagram of OTUs in Normal, Model, and HTD groups. C. Unweighted UPGMA cluster tree of three groups. D-F. Relative abundance analysis of dominant intestinal flora at the phylum, family, and genus levels in each group. G-I. Ternary diagram of dominant intestinal flora at the phylum, family, and genus levels in each group.

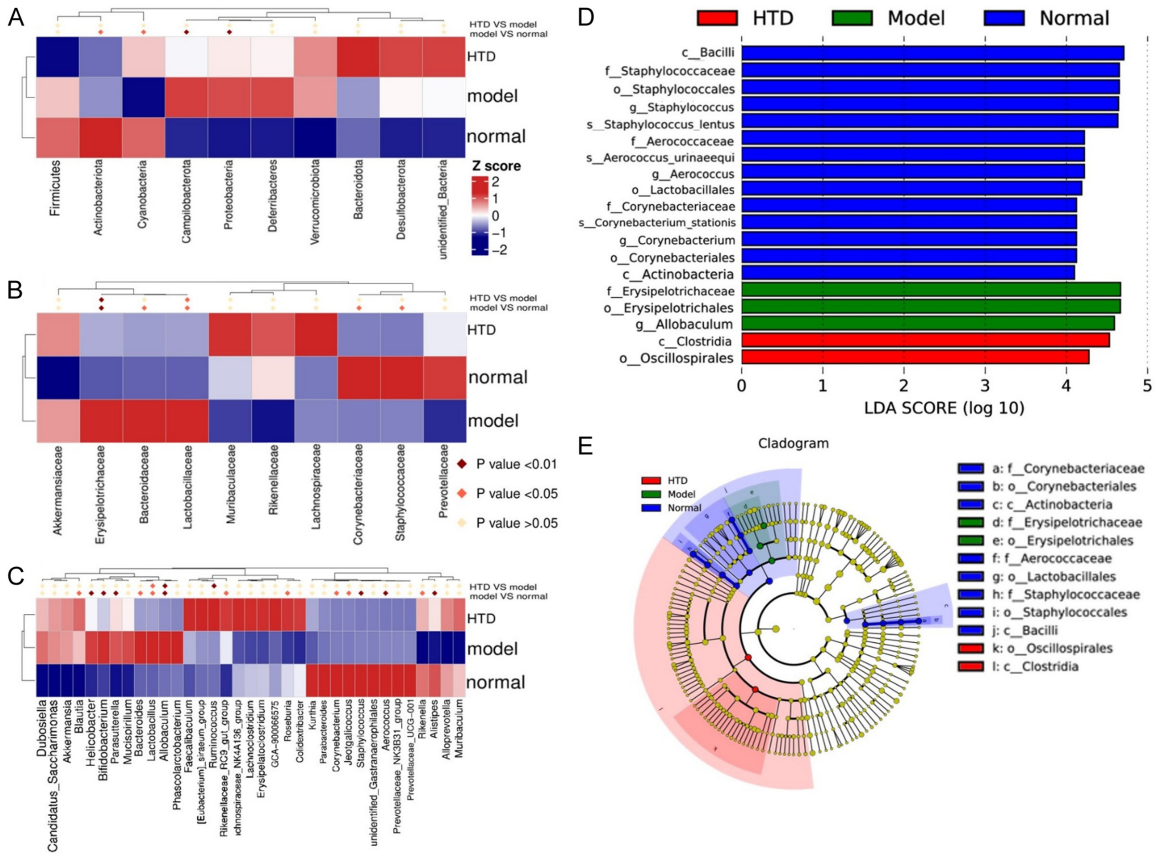

Figure 4. Differential bacteria identification in each group. A-C. MetaStat analysis heatmaps of gut flora at the phylum level, family level, and genus level, respectively. D. Linear discriminant analysis (LDA) scores. E. Cladogram-based LDA integrated with effect size (LEfSe).

Table 2 and **Figure 6A**, **6B** show that HTD significantly restored 14 differential metabolites in CDSD mice to levels similar to those in normal mice. **Figure 6C** shows the contents of the differential metabolites in each group. HTD treatment increased the levels of dihydroroseoside, 3-hydroxy-3-methylglutaric acid, arachidonic acid methyl ester, and LPC 2:0, whereas L-ascorbate, 19-nortestosterone, hexadecanedioic acid, jasmonic acid, 2-hydroxycaproic acid, 6 β-hydroxycortisol, 2-hydroxy-2-methylbutanoic acid, 23-nordeoxycholic acid, (+/-)9-HpODE, and prostaglandin B2 were decreased.

Pathway enrichment analysis showed that HTD mainly regulated ascorbate and aldarate metabolism, aldosterone synthesis and secretion, platelet activation, the hypoxia-inducible factor 1 (HIF-1) signaling pathway, inositol phosphate metabolism, phosphatidylinositol signaling system, galactose metabolism, and alpha-linolenic acid metabolism pathways of metabolite changes caused by modeling (**Figure 7A**, **7B**).

Associations between different genera and metabolites

To investigate whether the HTD-retraced metabolite was correlated with intestinal flora, Spearman's correlation between differential flora and differential metabolites at the genus level between groups was performed. The results showed a significant correlation between the three differential genera and 14 differential metabolites in the normal *vs.* model group (**Figure 8**). Some bacteria enriched in amino acids, such as Allobaculum, were found to be associated with L-ascorbate, 19-Nortestosterone, hexadecanedioic acid, jasmonic acid, 2-Hydroxycaproic acid, 2-Hydroxy-2-methylbutanoic acid, 23-Nordeoxycholic acid, (+/-)9-HpODE, prostaglandin B2, and 3-Hydroxy-3-methylglutaric acid, and decreased in abun-

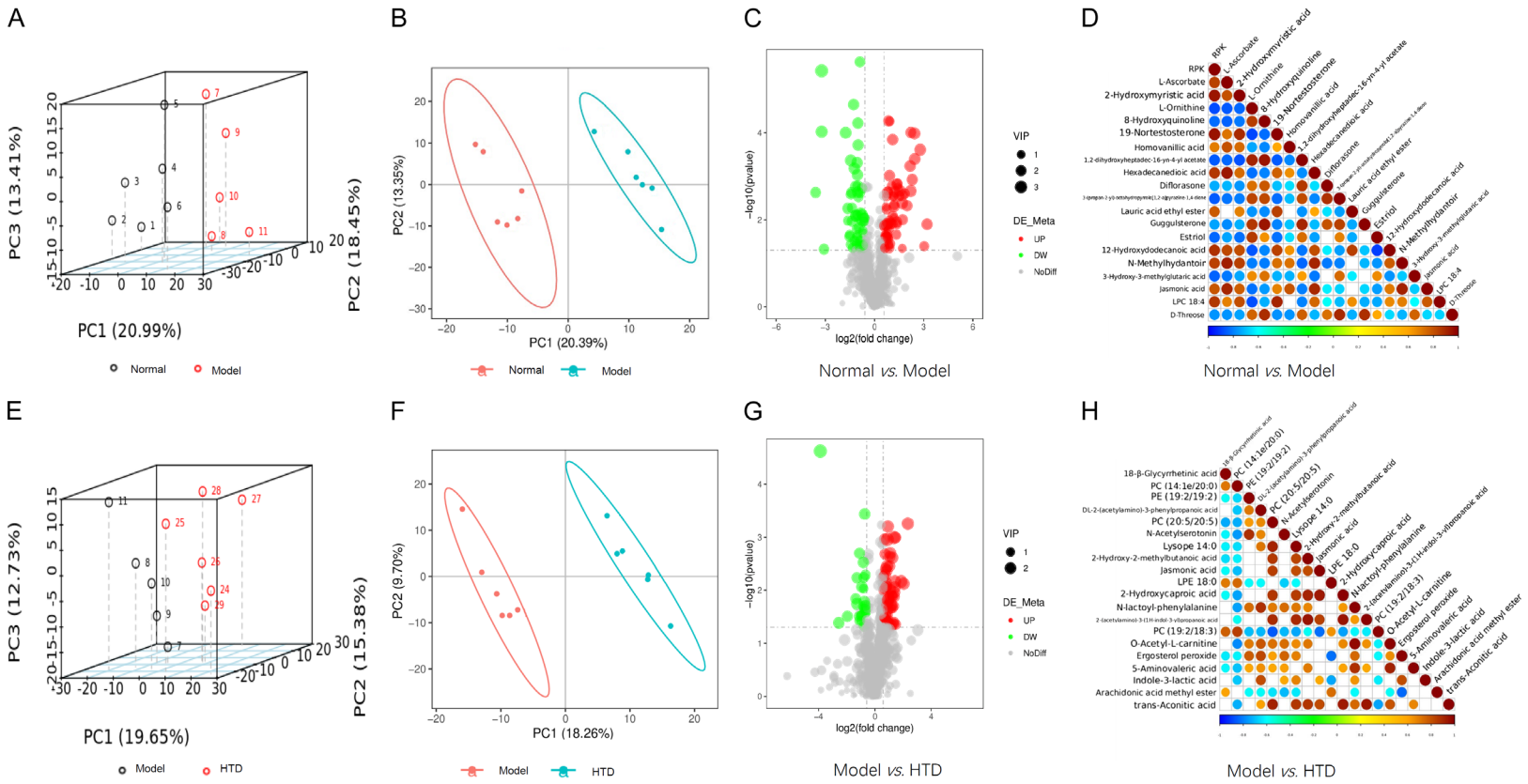

Figure 5. Overall metabolic characteristics of Normal, Model, and HTD groups. A, B, E, F. PLS-DA score plots and 3D PCA score plots demonstrate a complete separation of the serum samples among the groups. C, G. Volcano plots of metabolite distribution among the groups. D, H. Correlation of different metabolites among the groups.

Table 2. Biomarkers identified in CDSD mice and their trends of change afer intervention by HTD

No.	Name	Formula	RT [min]	m/z	Ion mode	Normal *vs.* Model				Model *vs.* HTD			
						FC	VIP	*P* value	Trend	FC	VIP	*P* value	Trend
1	L-Ascorbate	$C_6H_8O_6$	7.688	175.02443	neg	0.11	3.44	< 0.001	↓***	2.06	1.07	0.013	↑#
2	19-Nortestosterone	$C_{18}H_{26}O_2$	14.059	275.20026	pos	0.50	2.21	< 0.001	↓***	1.78	2.00	0.009	↑##
3	Hexadecanedioic acid	$C_{16}H_{30}O_4$	12.59	285.20685	neg	0.30	2.58	< 0.001	↓***	1.90	1.55	0.023	↑#
4	3-Hydroxy-3-methylglutaric acid	$C_6H_{10}O_5$	1.376	161.04549	neg	4.51	2.51	0.001	↑**	0.51	1.23	0.038	↓#
5	Jasmonic acid	$C_{12}H_{18}O_3$	13.388	211.13272	pos	0.43	2.55	0.001	↓**	2.11	2.30	0.002	↑##
6	2-Hydroxycaproic acid	$C_6H_{12}O_3$	4.126	131.07112	neg	0.59	1.85	0.002	↓**	1.66	1.78	0.002	↑##
7	Dihydroroseoside	$C_{19}H_{32}O_8$	11.057	387.20227	neg	4.64	2.59	0.002	↑**	0.46	1.48	0.031	↓#
8	6 β-Hydroxycortisol	$C_{21}H_{30}O_6$	11.757	361.20071	pos	0.32	2.18	0.005	↓**	2.18	1.36	0.022	↑#
9	2-Hydroxy-2-methylbutanoic acid	$C_5H_{10}O_3$	2.01	117.05566	neg	0.65	1.82	0.009	↓**	1.85	2.61	0.001	↑##
10	Arachidonic acid methyl ester	$C_{21}H_{34}O_2$	13.962	319.26138	pos	1.76	1.81	0.014	↑*	0.63	1.61	0.005	↓##
11	LPC 2:0	$C_{10}H_{22}NO_7P$	14.552	300.12683	pos	0.47	1.54	0.016	↓*	0.55	1.25	0.020	↓#
12	23-Nordeoxycholic acid	$C_{23}H_{38}O_4$	11.777	377.26935	neg	0.35	1.33	0.022	↓*	2.56	1.43	0.040	↑#
13	(+/-)9-HpODE	$C_{18}H_{32}O_4$	13.087	311.22244	neg	0.35	1.91	0.024	↓*	2.50	1.84	0.044	↑#
14	Prostaglandin B2	$C_{20}H_{30}O_4$	12.306	335.22116	pos	0.53	1.41	0.045	↓*	1.98	1.81	0.043	↑#

*P < 0.05, **P < 0.01, ***P < 0.001 Normal vs. Model group. #P < 0.05; ##P < 0.01 Model vs. HTD group.

dance after HTD treatment and was associated with LPC 2:0. Lactobacillus was associated with L-ascorbate, hexadecanedioic acid, 2-Hydroxycaproic acid, 2-Hydroxy-2-methylbutanoic acid, 23-Nordeoxycholic acid, (+/-)9-HpODE, and prostaglandin B2 but was decreased in abundance after HTD treatment and was associated with 23-Nordeoxycholic acid and prostaglandin B2. Ruminococcus was associated with L-ascorbate, hexadecanedioic acid, jasmonic acid, 2-Hydroxycaproic acid, 2-Hydroxy-2-methylbutanoic acid, 23-Nordeoxycholic acid, (+/-)9-HpODE, and prostaglandin B2, but it increased in abundance after HTD treatment and was associated with jasmonic acid and 3-Hydroxy-3-methylglutaric acid.

Discussion

Many studies have demonstrated that chronic diarrhea is closely related to intestinal flora disorders, including intestinal flora and fungal and viral imbalances, and is a popular research field for diarrhea [34, 35].

Huangtu decoction, a classic TCM, has been used to treat gastrointestinal bleeding, diarrhea, and other symptoms caused by spleen-yang deficiency for more than 2,000 years in China. The HPLC assay of the HTD extracts was showed that the main constituents are nucleosides, organic acid, flavones and alkaloids, (Figure S1). The compounds within HTD, such as polysaccharides from *Aconiti Lateralis Radix*, *Atractylodis Macrocephalae Rhizoma* and *Glycyrrhizae Radix et Rhizoma*, catalpol from *Rehmanniae Radix*, and baicalin from *Scutellariae Radix*, have been shown to regulate serum metabolites and microbiota composition, including those involved in inflammation regulation, gut barrier integrity, and neurotransmitter modulation. However, its mechanism of action has not been reported. This study clarified the mechanism of Huangtu decoction from the perspective of intestinal flora and host metabolism. We found that Huangtu decoction could reverse the abundance changes of Erysipelotrichaceae, Lactobacillus, Allobaculum, Lactobacillus, and Ruminococcus caused by modeling to a certain extent. Erysipelotrichaceae is considered to play an important role in gastrointestinal inflammation-related diseases because of its significant enrichment in colorectal cancer [36]. Many studies have also observed a significant increase in the abundance of Erysipelotrichaceae in IBD animals [37, 38], whereas HTD treatment decreased the abundance of Erysipelotrichaceae in CDSD mice. Ruminococcus was observed with an increased abundance in the gut microbiota of subjects with IBS compared to that in the normal group [39], while HTD treatment increased Ruminococcus in CDSD mice. These findings suggest that the warming spleen and relief of diarrhea effects of *Huangtu* decoction may be attributed to increasing the expression of beneficial bacteria and reducing the expression of harmful bacteria in the intestine.

A total of 14 differential metabolites related to the warming spleen and relief of diarrhea

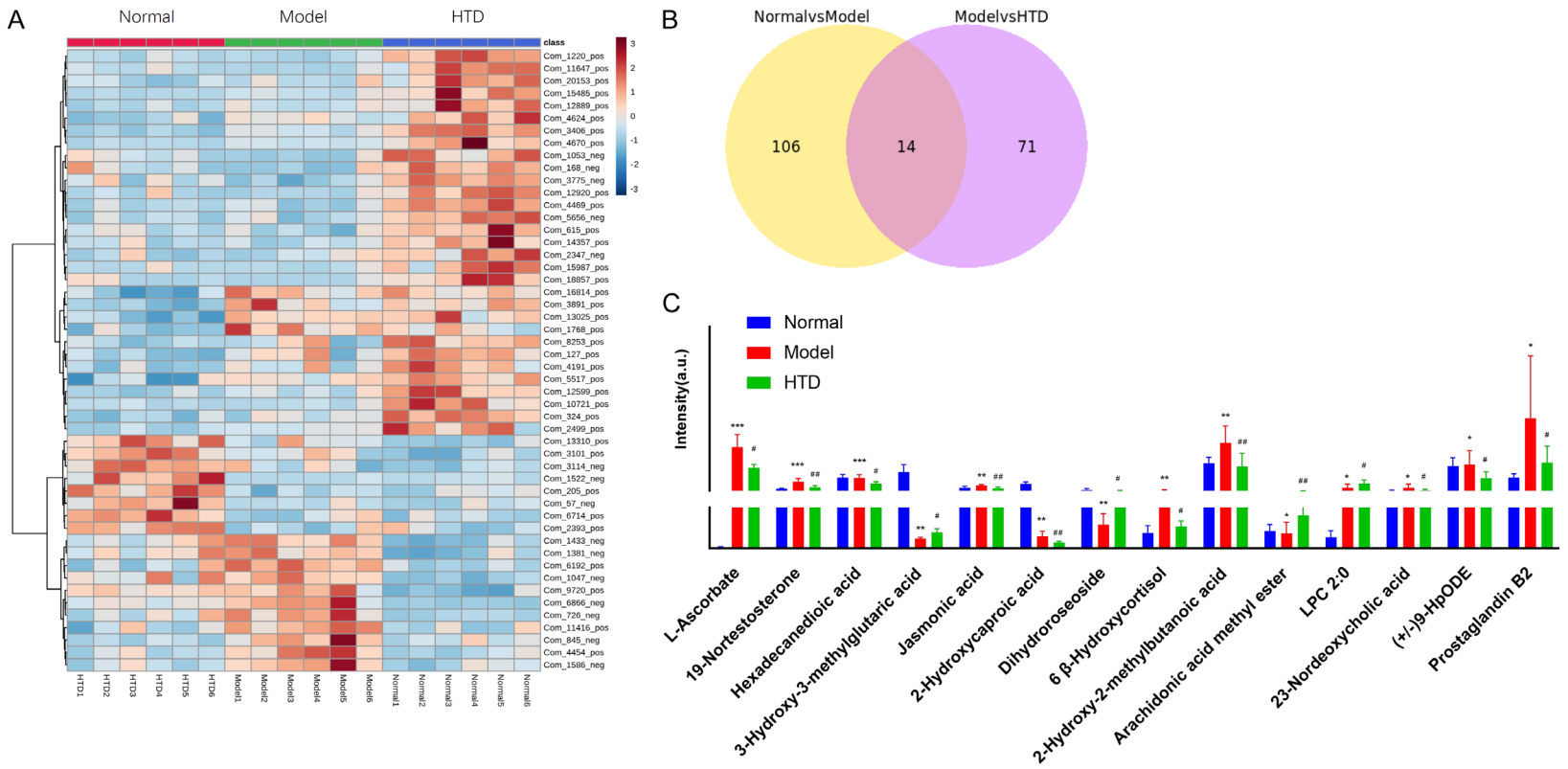

Figure 6. Effects of different treatments on serum metabolites in each group. A. Heatmap of differential metabolites. B. Venn diagram of differential metabolites of Normal group vs. Model group (yellow) and Model group vs. HTD group (pink). C. Bar graph of the differential metabolites in the different groups of serum. *P < 0.05, **P < 0.01, ***P < 0.001 vs. Normal group. #P < 0.05; ##P < 0.01 vs. Model group.

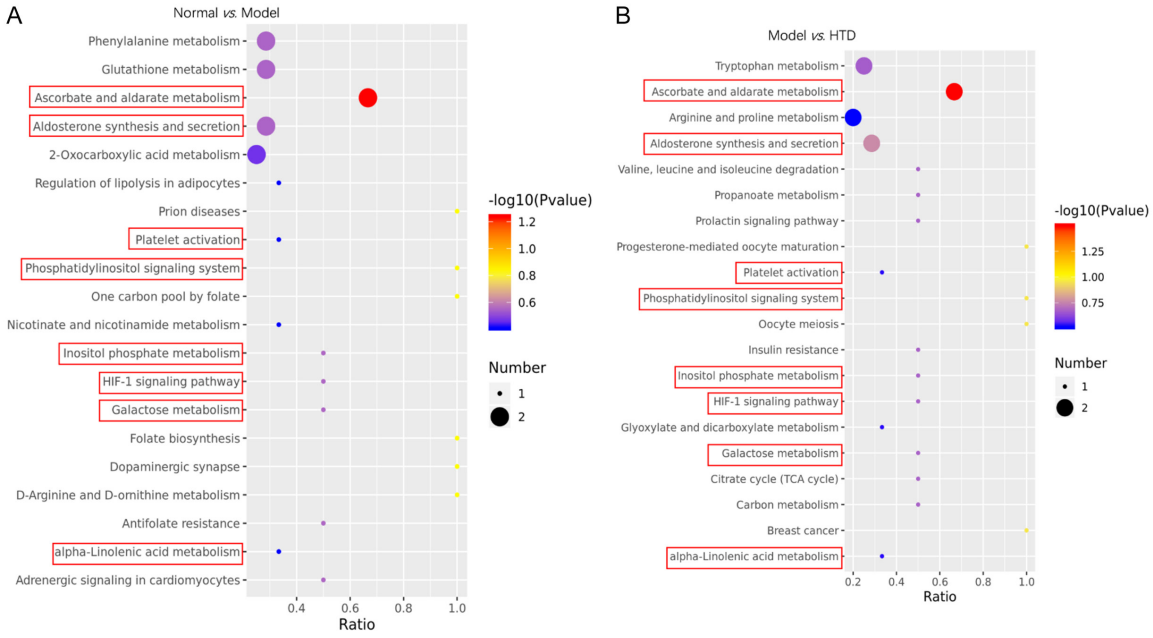

Figure 7. KEGG enrichment and pathway analysis. A. Normal *vs*. Model. B. Model *vs*. HTD.

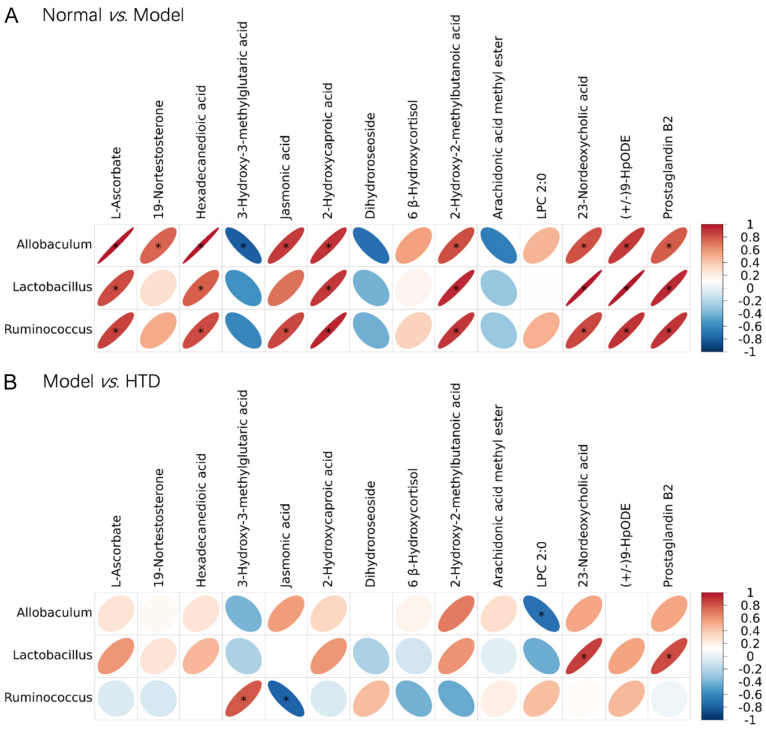

Figure 8. Correlation analysis between differential genera and metabolites. A. Normal *vs*. Model. B. Model *vs*. HTD. **P* value < 0.05.

effects of *Huangtu* decoction were identified by non-targeted metabolomics: dihydroroseoside, 3-hydroxy-3-methylglutaric acid, arachidonic acid methyl ester, LPC 2:0, L-ascorbate, 19-nortestosterone, hexadecanedioic acid, jasmonic acid, 2-hydroxycaproic acid, 6 β-hydroxycortisol, 2-hydroxy-2-methylbutanoic acid, 23-nordeoxycholic acid, (+/-)9-HpODE, and prostaglandin B2. The differential metabolites were enriched using KEGG. It was found that the main regulatory pathway was the HIF-1 signaling pathway, which produces a complex and rapid response to cell stress, injury, and inflammation, and can protect the intestinal mucosa [40-42]. In addition to promoting the adaptive response of the body to hypoxia, the HIF-1 pathway also plays a regulatory role in various cellular processes involved in immune and intestinal barrier function [43-45]. The HIF-1 pathway can increase the transcription of genes involved in wound repair, inflammation, cell permeability, and apoptosis (e.g., VEGF, eNOS, iNOS, and ITF), alleviate many aspects of the inflammation-injury cascade, and promote the expression of a series of barrier protection

genes, including TFF3/ITF, MUC-1, and CD73 [46, 47]. Therefore, it can be speculated that *Huangtu* decoction may increase HIF-1 expression and enhance the function of the intestinal barrier, reduce the production of proinflammatory cytokines and immune cell infiltration, and alleviate the inflammatory response of intestinal tissue.

Considering that intestinal flora can regulate metabolic reactions, a correlation between intestinal flora and serum metabolites was observed. The HTD-related intestinal floras were correlated with LPC 2:0, 23-Nordeoxycholic acid, Prostaglandin B2, jasmonic acid, and 3-Hydroxy-3-methylglutaric acid, while the other metabolites were not correlated with the bacteria. Therefore, it can be assumed that the changes in the content of LPC 2:0, 23-Nordeoxycholic acid, Prostaglandin B2, jasmonic acid, and 3-Hydroxy-3-methylglutaric acid were due to HTD treatment.

This study has several limitations. The sample size of each group of mice was small. A larger sample size of animal models and more verification experiments are needed to explore the mechanisms of HTD in CDSD treatment.

Conclusion

This study found that HTD exerted beneficial effects on CDSD mice by modulating the abnormal intestinal bacterial structure and affecting its metabolites. This is the first study to investigate the effect of HTD on the gut microbiome of CDSD mice and may provide new insight into the mechanisms of HTD.

Acknowledgements

The research was supported by the National Natural Science Foundation of China (Grant No. 82204970), and Project of Chengdu Women's and Children's Central Hospital (2022JC07).

Disclosure of conflict of interest

None.

Address correspondence to: Dr. Xiao Yang, Department of Obstetrics, Chengdu Women's and Children's Central Hospital, School of Medicine, University of Electronic Science and Technology of China, No. 1617 Riyue Anvenue, Chengdu 610091, Sichuan, China. E-mail: yangxiao0912@126.com

References

[1] Schiller LR, Pardi DS and Sellin JH. Chronic diarrhea: diagnosis and management. Clin Gastroenterol Hepatol 2017; 15: 182-193, e3.

[2] Alexander KA, Carzolio M, Goodin D and Vance E. Climate change is likely to worsen the public health threat of diarrheal disease in Botswana. Int J Environ Res Public Health 2013; 10: 1202-1230.

[3] Guerrant RL, DeBoer MD, Moore SR, Scharf RJ and Lima AA. The impoverished gut--a triple burden of diarrhoea, stunting and chronic disease. Nat Rev Gastroenterol Hepatol 2013; 10: 220-229.

[4] Troeger CE, Khalil IA, Blacker BF, Biehl MH, Albertson SB, Zimsen SRM, Rao PC, Abate D, Ahmadi A, Ahmed MLCB, Akal CG, Alahdab F, Alam N, Alene KA, Alipour V, Aljunid SM, Al-Raddadi RM, Alvis-Guzman N, Amini S, Anber NH, Anjomshoa M, Antonio CAT, Arabloo J, Aremu O, Atalay HT, Atique S, Avokpaho EFGA, Awad S, Awasthi A, Badawi A, Balakrishnan K, Banoub JAM, Barac A, Bassat Q, Bedi N, Bennett DA, Bhattacharyya K, Bhutta ZA, Bijani A, Car J, Carvalho F, Castañeda-Orjuela CA, Christopher DJ, Dandona L, Dandona R, Daryani A, Demeke FM, Deshpande A, Djalalinia S, Dubey M, Dubljanin E, Duken EE, El Sayed Zaki M, Endries AY, Fernandes E, Fischer F, Fullman N, Gardner WM, Geta B, Ghadiri K, Gorini G, Goulart AC, Guo Y, Hailu GB, Haj-Mirzaian A, Haj-Mirzaian A, Hamidi S, Hassen HY, Hoang CL, Hostiuc M, Hussain Z, Irvani SSN, James SL, Jha RP, Jonas JB, Karch A, Kasaeian A, Kassa TD, Kassebaum NJ, Kefale AT, Khader YS, Khan EA, Khan MN, Khang YH, Khoja AT, Kimokoti RW, Kisa A, Kisa S, Kissoon N, Kochhar S, Kosen S, Koyanagi A, Kuate Defo B, Kumar GA, Lal DK, Leshargie CT, Li S, Lodha R, Macarayan ERK, Majdan M, Mamun AA, Manguerra H, Melese A, Memish ZA, Mengistu DT, Meretoja TJ, Mestrovic T, Miazgowski B, Mirrakhimov EM, Moazen B, Mohammad KA, Mohammed S, Monasta L, Moore CE, Mosser JF, Mousavi SM, Murthy S, Mustafa G, Nazari J, Nguyen CT, Nguyen LH, Nisar MI, Nixon MR, Ogbo FA, Okoro A, Olagunju AT, Olagunju TO, P A M, Pakhale S, Postma MJ, Qorbani M, Quansah R, Rafiei A, Rahim F, Rahimi-Movaghar V, Rai RK, Rezai MS, Rezapour A, Rios-Blancas MJ, Ronfani L, Rosettie K, Rothenbacher D, Safari S, Saleem Z, Sambala EZ, Samy AM, Santric Milicevic MM, Sartorius B, Sawhney M, Seyedmousavi S, Shaikh MA, Sheikh A, Shigematsu M, Smith DL, Soriano JB, Sreeramareddy CT, Stanaway JD, Sufiyan MB, Teklu TGE, Temsah MH, Tessema B, Tran BX, Tran KB, Ullah I, Updike

RL, Vasankari TJ, Veisani Y, Wada FW, Waheed Y, Weaver M, Wiens KE, Wiysonge CS, Yimer EM, Yonemoto N, Zaidi Z, Zar HJ, Zarghi A, Lim SS, Vos T, Mokdad AH, Murray CJL, Kyu HH, Hay SI and Reiner RC. Quantifying risks and interventions that have affected the burden of diarrhoea among children younger than 5 years: an analysis of the Global Burden of Disease Study 2017. Lancet Infect Dis 2020; 20: 37-59.

[5] SchillerLR. Evaluation of chronic diarrhea and irritable bowel syndrome with diarrhea in adults in the era of precision medicine. Am J Gastroenterol 2018; 113: 660-669.

[6] Zuo T and Ng SC. The gut microbiota in the pathogenesis and therapeutics of inflammatory bowel disease. Front Microbiol 2018; 9: 2247.

[7] Rhoades N, Barr T, Hendrickson S, Prongay K, Haertel A, Gill L, Garzel L, Whiteson K, Slifka M and Messaoudi I. Maturation of the infant rhesus macaque gut microbiome and its role in the development of diarrheal disease. Genome Biol 2019; 20: 173.

[8] Kim HS, Whon TW, Sung H, Jeong YS, Jung ES, Shin NR, Hyun DW, Kim PS, Lee JY, Lee CH and Bae JW. Longitudinal evaluation of fecal microbiota transplantation for ameliorating calf diarrhea and improving growth performance. Nat Commun 2021; 12:161.

[9] Ianiro G, Rossi E, Thomas AM, Schinzari G, Masucci L, Quaranta G, Settanni CR, Lopetuso LR, Armanini F, Blanco-Miguez A, Asnicar F, Consolandi C, Iacovelli R, Sanguinetti M, Tortora G, Gasbarrini A, Segata N and Cammarota G. Faecal microbiota transplantation for the treatment of diarrhoea induced by tyrosine-kinase inhibitors in patients with metastatic renal cell carcinoma. Nat Commun 2020; 11: 4333.

[10] Zhang Z, Yang S, Lin X, Huang Y, Wei X, Zhou J, Li R, Deng B and Fu C. Metabolomics of Spleen-Yang deficiency syndrome and the therapeutic effect of Fuzi Lizhong pill on regulating endogenous metabolism. J Ethnopharmacol 2021; 278: 114281.

[11] Liu X, Tong X, Zou Y, Lin X, Zhao H, Tian L, Jie Z, Wang Q, Zhang Z, Lu H, Xiao L, Qiu X, Zi J, Wang R, Xu X, Yang H, Wang J, Zong Y, Liu W, Hou Y, Zhu S, Jia H and Zhang T. Mendelian randomization analyses support causal relationships between blood metabolites and the gut microbiome. Nat Genet 2022; 54: 52-61.

[12] Jia Q, Wang L, Zhang X, Ding Y, Li H, Yang Y, Zhang A, Li Y, Lv S and Zhang J. Prevention and treatment of chronic heart failure through traditional Chinese medicine: role of the gut microbiota. Pharmacol Res 2020; 151: 104552.

[13] Liang B and Gu N. Traditional Chinese medicine for coronary artery disease treatment: clinical evidence from randomized controlled trials. Front Cardiovasc Med 2021; 8: 702110.

[14] Deyrup ST, Stagnitti NC, Perpetua MJ and Wong-Deyrup SW. Drug discovery insights from medicinal beetles in traditional Chinese medicine. Biomol Ther (Seoul) 2021; 29: 105-126.

[15] Peng W, Chen Y, Tumilty S, Liu L, Luo L, Yin H and Xie Y. Paeoniflorin is a promising natural monomer for neurodegenerative diseases via modulation of Ca2+ and ROS homeostasis. Curr Opin Pharmacol 2022; 62: 97-102.

[16] Yan J, Miao ZW, Lu J, Ge F, Yu LH, Shang WB, Liu LN and Sun ZG. Acupuncture plus Chinese herbal medicine for irritable bowel syndrome with diarrhea: a systematic review and meta-analysis. Evid Based Complement Alternat Med 2019; 2019: 7680963.

[17] Zhen Z, Xia L, You H, Jingwei Z, Shasha Y, Xinyi W, Wenjing L, Xin Z and Chaomei F. An integrated gut microbiota and network pharmacology study on Fuzi-Lizhong pill for treating diarrhea-predominant irritable bowel syndrome. Front Pharmacol 2021; 12: 746923.

[18] Guan Z, Zhao Q, Huang Q, Zhao Z, Zhou H, He Y, Li S and Wan S. Modified Renshen Wumei Decoction alleviates intestinal barrier destruction in rats with diarrhea. J Microbiol Biotechnol 2021; 31: 1295-1304.

[19] Qu Q, Yang F, Zhao C, Liu X, Yang P, Li Z, Han L and Shi X. Effects of fermented ginseng on the gut microbiota and immunity of rats with antibiotic-associated diarrhea. J Ethnopharmacol 2021; 267: 113594.

[20] Xie Y, Zhan X, Tu J, Xu K, Sun X, Liu C, Ke C, Cao G, Zhou Z and Liu Y. Atractylodes oil alleviates diarrhea-predominant irritable bowel syndrome by regulating intestinal inflammation and intestinal barrier via SCF/c-kit and MLCK/MLC2 pathways. J Ethnopharmacol 2021; 272: 113925.

[21] Zhang BX, Qi XJ and Cai Q. Metabolomic study of raw and bran-fried Atractylodis Rhizoma on rats with spleen deficiency. J Pharm Biomed Anal 2020; 182: 112927.

[22] Zhang Z, Yang S, Lin X, Huang Y, Wei X, Zhou J, Li R, Deng B and Fu C. Metabolomics of Spleen-Yang deficiency syndrome and the therapeutic effect of Fuzi Lizhong pill on regulating endogenous metabolism. J Ethnopharmacol 2021; 278: 114281.

[23] Chen W, He L, Zhong L, Sun J, Zhang L, Wei D and Wu C. Identification of active compounds and mechanism of Huangtu decoction for the treatment of ulcerative colitis by network pharmacology combined with experimental verification. Drug Des Devel Ther 2021; 15: 4125-4140.

[24] Wang Z, Peng Y and Li XB. Effect of sijunzi decoction on the intestinal flora disturbance in two rat models of Pi-deficiency syndrome. Zhongguo Zhong Xi Yi Jie He Za Zhi 2009; 29: 825-829.

[25] Zhao YP, Tang XD, Bian ZX, Wang FY, Yang JQ, Su M and Wang W. Preliminary study of establishing and assessing IBS-D model rats of gan stagnation and Pi deficiency syndrome. Zhongguo Zhong Xi Yi Jie He Za Zhi 2013; 33: 1507-1514.
[26] Jia LQ, Zhen BX, Xu Ying and Yang GL. Study on serum metabolite profiling in Pi-deficiency rats based on LC-MS technique. Zhongguo Zhong Xi Yi Jie He Za Zhi 2016; 36: 359-365.
[27] Yi YL, Li Y, Guo S, Yan H, Ma XF, Tao WW, Shang EX, Niu Y, Qian DW and Duan JA. Elucidation of the reinforcing spleen effect of jujube fruits based on metabolomics and intestinal flora analysis. Front Cell Infect Microbiol 2022; 12: 847828.
[28] Magoč T and Salzberg SL. FLASH: fast length adjustment of short reads to improve genome assemblies. Bioinformatics 2011; 27: 2957-2963.
[29] Caporaso JG, Kuczynski J, Stombaugh J, Bittinger K, Bushman FD, Costello EK, Fierer N, Peña AG, Goodrich JK, Gordon JI, Huttley GA, Kelley ST, Knights D, Koenig JE, Ley RE, Lozupone CA, McDonald D, Muegge BD, Pirrung M, Reeder J, Sevinsky JR, Turnbaugh PJ, Walters WA, Widmann J, Yatsunenko T, Zaneveld J and Knight R. QIIME allows analysis of high-throughput community sequencing data. Nat Methods 2010; 7: 335-336.
[30] Edgar RC. UPARSE: highly accurate OTU sequences from microbial amplicon reads. Nat Methods 2013; 10: 996-998.
[31] Quast C, Pruesse E, Yilmaz P, Gerken J, Schweer T, Yarza P, Peplies J and Glöckner FO. The SILVA ribosomal RNA gene database project: improved data processing and web-based tools. Nucleic Acids Res 2013; 41: D590-596.
[32] Barri T and Dragsted LO. UPLC-ESI-QTOF/MS and multivariate data analysis for blood plasma and serum metabolomics: effect of experimental artefacts and anticoagulant. Anal Chim Acta 2013; 768: 118-128.
[33] Wen B, Mei Z, Zeng C and Liu S. metaX: a flexible and comprehensive software for processing metabolomics data. BMC Bioinformatics 2017; 18: 183.
[34] Li Y, Xia S, Jiang X, Feng C, Gong S, Ma J, Fang Z, Yin J and Yin Y. Gut microbiota and diarrhea: an updated review. Front Cell Infect Microbiol 2021; 11: 625210.
[35] Yang S, Liu Y, Yang N, Lan Y, Lan W, Feng J, Yue B, He M, Zhang L, Zhang A, Price M, Li J and Fan Z. The gut microbiome and antibiotic resistome of chronic diarrhea rhesus macaques (Macaca mulatta) and its similarity to the human gut microbiome. Microbiome 2022; 10: 29.
[36] Kaakoush NO. Insights into the role of erysipelotrichaceae in the human host. Front Cell Infect Microbiol 2015; 5: 84.
[37] Craven M, Egan CE, Dowd SE, McDonough SP, Dogan B, Denkers EY, Bowman D, Scherl EJ and Simpson KW. Inflammation drives dysbiosis and bacterial invasion in murine models of ileal Crohn's disease. PLoS One 2012; 7: e41594.
[38] Schaubeck M, Clavel T, Calasan J, Lagkouvardos I, Haange SB, Jehmlich N, Basic M, Dupont A, Hornef M, von Bergen M, Bleich A and Haller D. Dysbiotic gut microbiota causes transmissible Crohn's disease-like ileitis independent of failure in antimicrobial defence. Gut 2016; 65: 225-237.
[39] Sabo CM and Dumitrascu DL. Microbiota and the irritable bowel syndrome. Minerva Gastroenterol (Torino) 2021; 67: 377-384.
[40] Hirota SA, Beck PL and MacDonald JA. Targeting hypoxia-inducible factor-1 (HIF-1) signaling in therapeutics: implications for the treatment of inflammatory bowel disease. Recent Pat Inflamm Allergy Drug Discov 2009; 3: 1-16.
[41] Hirota SA, Fines K, Ng J, Traboulsi D, Lee J, Ihara E, Li Y, Willmore WG, Chung D, Scully MM, Louie T, Medlicott S, Lejeune M, Chadee K, Armstrong G, Colgan SP, Muruve DA, MacDonald JA and Beck PL. Hypoxia-inducible factor signaling provides protection in Clostridium difficile-induced intestinal injury. Gastroenterology 2010; 139: 259-69, e3.
[42] Yin J, Ren Y, Yang K, Wang W, Wang T, Xiao W and Yang H. The role of hypoxia-inducible factor 1-alpha in inflammatory bowel disease. Cell Biol Int 2022; 46: 46-51.
[43] Hellwig-Bürgel T, Stiehl DP, Wagner AE, Metzen E and Jelkmann W. Review: hypoxia-inducible factor-1 (HIF-1): a novel transcription factor in immune reactions. J Interferon Cytokine Res 2005; 25: 297-310.
[44] Cummins EP, Seeballuck F, Keely SJ, Mangan NE, Callanan JJ, Fallon PG and Taylor CT. The hydroxylase inhibitor dimethyloxalylglycine is protective in a murine model of colitis. Gastroenterology 2008; 134: 156-165.
[45] Robinson A, Keely S, Karhausen J, Gerich ME, Furuta GT and Colgan SP. Mucosal protection by hypoxia-inducible factor prolyl hydroxylase inhibition. Gastroenterology 2008; 134: 145-155.
[46] Karhausen J, Furuta GT, Tomaszewski JE, Johnson RS, Colgan SP and Haase VH. Epithelial hypoxia-inducible factor-1 is protective in murine experimental colitis. J Clin Invest 2004; 114: 1098-1106.
[47] Flück K, Breves G, Fandrey J and Winning S. Hypoxia-inducible factor 1 in dendritic cells is crucial for the activation of protective regulatory T cells in murine colitis. Mucosal Immunol 2016; 9: 379-390.

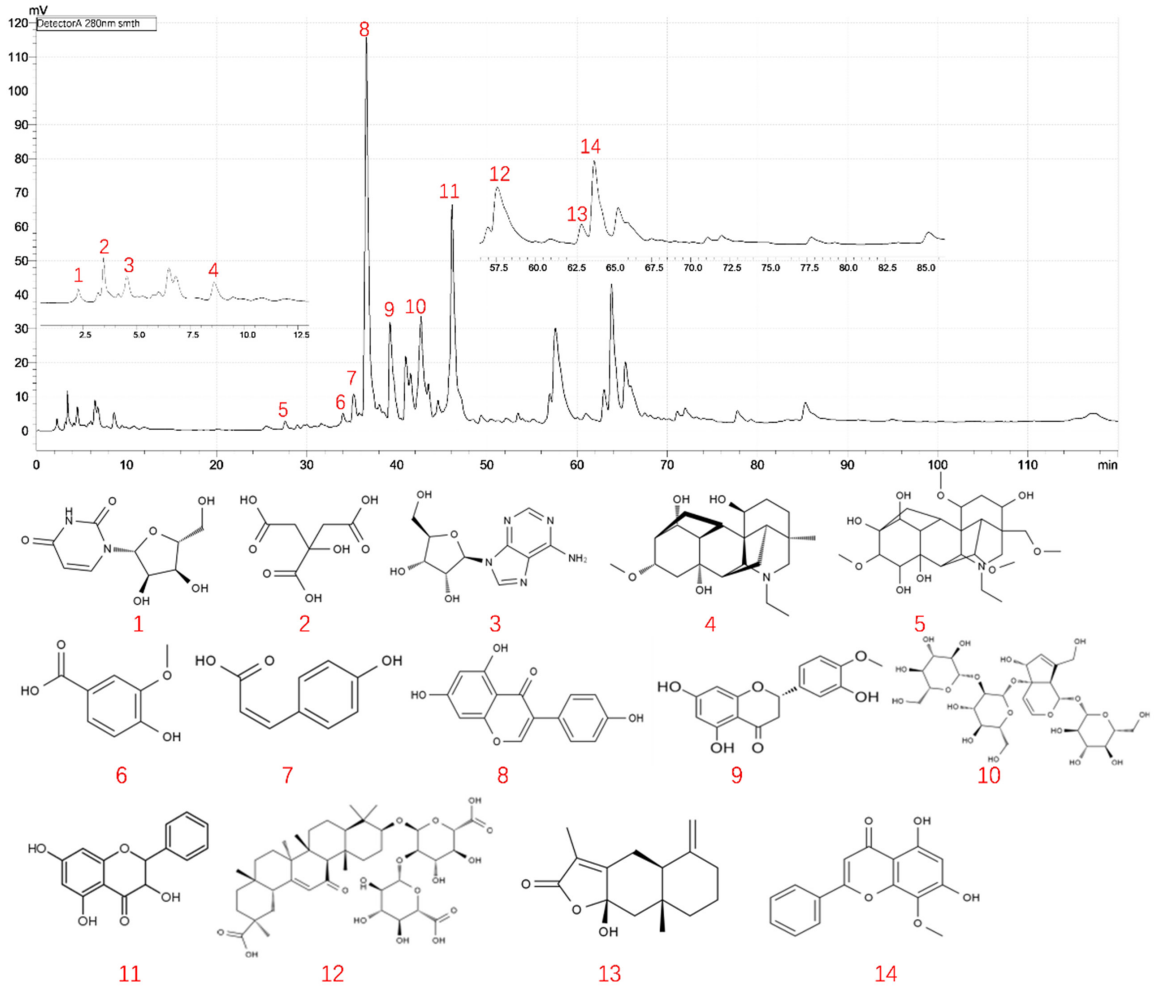

Figure S1. HPLC chromatograms of HTD extracts. Uridine (1), Citric acid (2), Adenosine (3), Karakoline (4), Aconine (5), Vanillic acid (6), P-coumaric acid (7), Genistein (8), Hesperetin (9), Rehmannioside (10), Pinobanksin (11), Glycyrrhizic acid (12), Atractylenolide III (13), Wogonin (14).